eprints@whiterose.ac.uk
https://eprints.whiterose.ac.uk/

Stability, Interfacial Structure, and Gastrointestinal Digestion of β-Carotene-Loaded Pickering Emulsions Co-stabilized by Particles, a Biopolymer, and a Surfactant

Yang Wei[a,b], Dan Zhou[a], Alan Mackie[b], Shufang Yang[a], Lei Dai[a], Liang Zhang[a], Like Mao[a], Yanxiang Gao[a*]

[a] Key Laboratory of Healthy Beverages, China National light Industry Council, College of Food Science & Nutritional Engineering, China Agricultural University, Beijing 100083, P. R. China

[b] Food Colloids and Processing Group, School of Food Science and Nutrition, University of Leeds, Leeds, LS2 9JT, UK

Abstract

Novel Pickering emulsions were stabilized by complex interfaces in the presence of zein colloidal particles (ZCPs), propylene glycol alginate (PGA), and rhamnolipid (Rha) for delivery of β-carotene. The influence of the particle–surfactant, particle–biopolymer, and particle–biopolymer–surfactant mixed interfaces on the physiochemical properties and digestion fate of Pickering emulsions was investigated. It is the first time that three different types of emulsifiers have been used to synergistically stabilize food Pickering emulsions for delivery of lipophilic nutraceuticals. The physicochemical stability, microstructure, rheological properties, and in vitro gastrointestinal digestion of Pickering emulsions were controlled by the addition sequence and mass ratio of multiple stabilizers, which showed the enhanced stability and delayed lipid digestion of the particle–biopolymer–surfactant-stabilized Pickering emulsions. After encapsulation into Pickering emulsions, the retention rate of β-carotene increased 2-fold under UV radiation for 8 h. The coexistence of ZCPs, PGA, and Rha could induce the competitive displacement, multilayer deposition, and interparticle network at the interface. The combination of particles, a biopolymer, and a surfactant delayed the lipolysis during in vitro gastrointestinal tract. By modulating the interfacial composition, the release rate of free fatty acids from Pickering emulsions was reduced from 19.46% to 2.83% through different mechanisms. The novel Pickering emulsion could be incorporated in foods as well as pharmaceuticals for controlled lipid digestion or targeted nutrient delivery purposes.
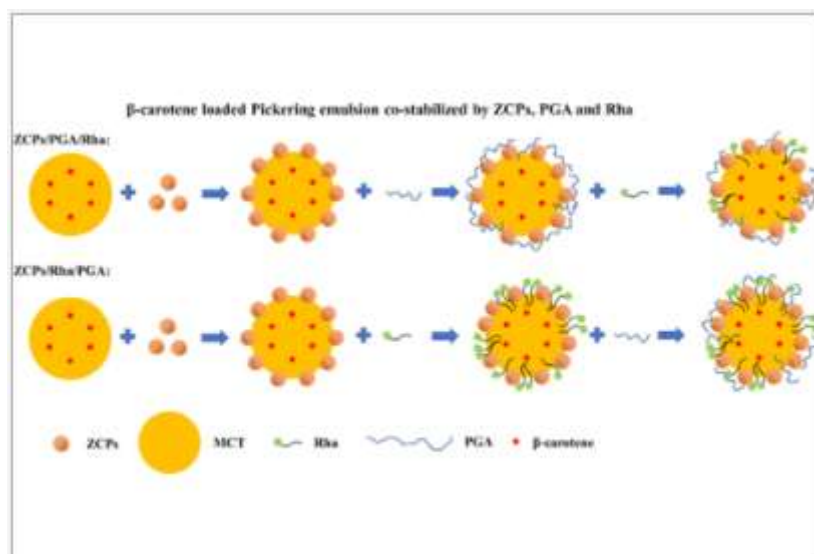
1. Introduction

Conventional emulsions are stabilized by surfactants or biopolymers. Owing to their low molecular weight, surfactants such as phospholipids and saponins can swiftly occupy the droplet surface and efficiently reduce the interfacial tension, which decrease the free energy of whole systems. (1) Although the adsorption rate of biopolymers (proteins and polysaccharides) onto the interface is lower than that of surfactants, they can provide better steric stability of droplets and their adsorption is less reversible. (2) Nevertheless, both biosurfactants and biopolymers have their limitations for practical application. Fluctuations in pH and ionic strength may lead to emulsion coalescence. This is because the electrostatic screening caused by increased ionic strength or decrease in charge caused by changes in pH may alter the interfacial layer, thus weakening interdroplet repulsion. (1) During the digestion of emulsions, the surface-active components secreted into the gastrointestinal tract (GIT) (bile salts and lipase/co-lipase) and produced by the digestion process (peptides and free fatty acids) may change the interfacial composition of lipid droplets and alter lipid digestion and nutrient absorption. (3,4)

The overwhelming Pickering emulsions in the food research are generally stabilized by colloidal particles prepared from biodegradable materials. An appropriate interfacial wettability of particles can promote the adsorption of particles at the interface. (5) Compared to traditional emulsions, the adsorption of particles at the interface is usually irreversible owing to their much higher desorption energy (up to thousands of kT). In recent years, an increasing number of studies have reported on the development of natural colloidal particles to stabilize Pickering emulsions, which prevent coalescence with a solid layer. (6–8) Nevertheless, the real interface of emulsions often contains mixtures of emulsifiers and particles with different compositions, e.g., particle–polymer, particle–surfactant, and polymer–surfactant. (1,3,9,10) There are many possibilities for the formation of complex interfaces, which are mainly classified as co-adsorption, complexation, and layer-by-layer deposition. (11–13) The ability of emulsifiers or particles to modulate the stability, functionality, and digestibility of emulsions can be improved by combination with other components. Murray et al. (2011) investigated the mechanism of the combination of proteins and cellulose particles or starch particles to stabilize emulsions. (14) Li and McClements (2011) reported the inhibition of lipolysis of protein-stabilized emulsions by the addition of different low-molecular-weight emulsifiers. (15) Our recent studies investigated the synergism of particles and individual proteins, polysaccharides, or surfactants in improving the stability of emulsions and controlling their lipolysis and nutrient bioaccessibility. (3,13,16) However, in the food colloid system, the effect of the complex interfaces composed of particles, biopolymers, and surfactants on the stability and digestion behavior of Pickering emulsions has never been reported. The purpose of this study was to prepare Pickering emulsions co-stabilized by particles, polysaccharides, and surfactants for delivery of β-carotene on the basis of previous work and explore the effects of different addition sequences and mass ratios of mixed stabilizers on the functional attributes of Pickering emulsions.

Zein is a distinct amphiphilic plant protein and can be self-assembled into colloidal particles owing to its inherent hydrophobicity, with a proportion of more than 50% hydrophobic amino acids. (17) In recent years, zein-based nanoparticles have been widely used for delivery of nutraceuticals and stabilization of Pickering emulsions. (8,17,18) PGA (propylene glycol alginate) is a unique polysaccharide with strong surface activity, which is obtained by esterification of sodium alginate and different proportions of propylene glycol. (18) Rha is a microbial surfactant, which is widely utilized to prepare nanoemulsions with the aid of external forces. (19) Due to its surface activity, Rha can rapidly adsorb onto the surface of droplets and reduce the interfacial intension. (19,20)

In this study, we selected β-carotene as a model lipophilic nutrient to be incorporated into the lipid phase. The β-carotene-loaded Pickering emulsions were stabilized by a combination of ZCPs, PGA, and Rha. The structural properties of Pickering emulsions were characterized by particle sizing, zeta-potential, confocal laser scanning microscopy (CLSM), and cryo-scanning electronic microscopy (cryo-SEM). Rheological properties and physicochemical stability of Pickering emulsions were tested under various environmental stresses. Furthermore, the *in vitro* digestion behavior of Pickering emulsions in the simulated GIT was investigated to assess the lipolysis and bioaccessibility of β-carotene. This study provided a theoretical basis for the application of the particle–polymer–surfactant complex interface-stabilized Pickering emulsions in enhancing the stability of emulsions and nutrients and modulating their digestion behavior.

2. Materials and Methods

2.1. Materials

Zein (protein content: 91.3%), lipase (pack size: L3126), and bile salts (pack size: 48305) were purchased from Sigma-Aldrich (USA). It has been reported that lipase activity is 100–500 units/mg protein (using olive oil). The bile salts are composed of 50% deoxycholic acid sodium salt and 50% cholic acid sodium salt. Propylene glycol alginate (PGA) (degree of esterification: 87.9%) was kindly donated by Hanjun Sugar Industry Co. Ltd. (Shanghai, China). Curcumin (98%) was purchased from China National Medicine Group Shanghai Corporation (Shanghai, China). Medium-chain triglycerides (MCT, Miglyol 812N) were purchased from Musim Mas (Medan, Indonesia). β-Carotene suspension (30% by mass β-carotene in sunflower oil) was supplied by Xinchang Pharmaceutical Company, Ltd. (Xinchang, Zhejiang, China). Rhamnolipid (purity, ≥90%) was obtained from Parnell Biological Technology Co. Ltd. (Shaanxi, China). Absolute ethanol (99.99%), solid sodium hydroxide, and liquid hydrochloric acid (36%, w/w) were obtained from Eshowbokoo Biological Technology Co., Ltd. (Beijing, China). All other chemical agents were of analytical grade.

2.2. Preparation of Particle Suspensions and PGA and Rha Solutions

Zein colloidal particles (ZCPs) were prepared by the emulsification–evaporation method. (18) Briefly, 4.5 g of zein was dissolved in 450 mL of 70% (v/v) aqueous ethanol solution and stirred at 600 rpm overnight at 25 °C until its complete dissolution. The solution was further homogenized for two cycles at 75 MPa (Niro-Soavi Panda, Parma, Italy). Thereafter, ethanol in the solution was removed with a rotary evaporator at 45 °C for 25 min and the remaining volume was set to around 100 mL. The sample was diluted with pH-adjusted water (pH 4.0) to 150 mL. The ZCP suspension was centrifuged (Sigma 3k15, Germany) at 3000 rpm for 10 min to separate large particles and aggregates if any. Finally, the supernatant obtained was adjusted to pH 4.0 using 0.5 M HCl solution. Part of the ZCP suspension was placed at 5 °C for further analysis and the other part was freeze-dried for 72 h to obtain a powder sample. In brief, 1.00% (w/v) PGA and Rha solutions were prepared through dissolving 1.0 g of PGA and Rha powder into 100 mL of deionized water overnight at 25 °C and adjusted to pH 4.0 by 0.5 M HCl solution.

2.3. Preparation of β-Carotene-Loaded Pickering Emulsions Co-stabilized by ZCPs, PGA, and Rha

β-Carotene suspension (20 g) was dissolved in MCT oil (180 g) at 140 °C for 10 s to form an oil phase (3.0 wt % β-carotene).

2.3.1. Method I

The primary emulsion was prepared by mixing 7.0 g of ZCP (3.0%, w/v) suspension with 15 g of oil phase at a speed of 18,000 rpm by using a blender (Ultra Turrax, model T25, IKA Labortechnic, Staufen,

Germany). After the complete dispersion of oil phase, the mixture was further homogenized for another 5 min. Secondary emulsions were fabricated by mixing the primary emulsion with 1, 2, 3..., 7 g of PGA solution (1.0%, w/v) and homogenized under the same condition. Final emulsions were fabricated by mixing the secondary emulsion with 7, 6, 5..., 1 g of Rha solution (1.0%, w/v), respectively, and homogenized under the same condition, which set the mass ratios of PGA to Rha as 1:7, 2:6, 3:5; 4:4, 5:3, 6:2, and 7:1, respectively. The Pickering emulsions were termed as 1P7R, 2P6R, 3P5R, 4P4R, 5P3R, 6P2R, and 7P1R according to the mass ratios of PGA to Rha. The pH of fresh emulsions was adjusted to 4.0 using 0.5 M HCl solution.

2.3.2. Method II

The primary emulsion was prepared by homogenizing 7.0 g of ZCP (3.0%, w/v) suspension with 15 g of oil phase through the same procedure as aforementioned. Secondary emulsions were fabricated by mixing the primary emulsion with 1, 2, 3..., 7 g of Rha solution (1.0%, w/v) and homogenized under the same condition. Final emulsions were fabricated by mixing the secondary emulsions with 7, 6, 5..., 1 g of PGA solution (1.0%, w/v), respectively, and homogenized under the same condition, enabling the mass ratios of Rha to PGA to be 1:7, 2:6, 3:5; 4:4, 5:3, 6:2, and 7:1, respectively. The Pickering emulsions were termed as 1R7P, 2R6P, 3R5P, 4R4P, 5R3P, 6R2P, and 7R1P according to the mass ratios of Rha to PGA. The pH of fresh emulsions was adjusted to 4.0 using 0.5 M HCl solution.

2.3.3. Control Groups

The Pickering emulsion was prepared by homogenizing 15.0 g of ZCP (3.0%, w/v) suspension with 15.0 g of oil phase through the same procedure as aforementioned and termed as ZCPs.

The primary emulsion was prepared by homogenizing 7.0 g of ZCP (3.0%, w/v) suspension with 15 g of oil phase through the same procedure as aforementioned. Secondary emulsion was fabricated by homogenizing the primary emulsion with 8 g of PGA solution (1.0%, w/v) and termed as ZCPs/PGA.

The primary emulsion was prepared by homogenizing 7.0 g of ZCP (3.0%, w/v) suspension with 15 g of oil phase through the same procedure as aforementioned. Secondary emulsion was fabricated by homogenizing the primary emulsion with 8 g of Rha solution (1.0%, w/v) and termed as ZCPs/Rha.

2.4. Particle Size, Zeta-Potential, and Wettability Measurements of Zein Colloidal Particles (ZCPs)

The particle size (Z-average size) and zeta-potential of ZCPs were analyzed using a Zetasizer (Nano-ZS90, Malvern Instruments Ltd., Worcestershire, UK) with a DTS1060 cuvette and the scattering angle was fixed at 90°. The sample was diluted 10 times with distilled water (pH 4.0) to avoid a multiple light scattering effect. Thereafter, the sample was adjusted to pH 4.0 to determine the particle size and zeta-potential. The refractive index (RI) of the material and dispersant was 1.59 and 1.33. The particle size was calculated using the Stokes–Einstein equation, and the average particle size was reported in the distribution of intensity. The zeta-potential of particles was obtained using the Smoluchowski model through electrophoretic mobility measurement. (21) All measurements were conducted in triplicate.

The contact angle ($\theta_{o/w}$) of ZCPs was determined with an OCA 20 AMP (Dataphysics Instruments GmbH, Germany) by the method described in our previous study. (16) The powder obtained from freeze-dried ZCPs was compressed to a thin tablet with a thickness of 2 mm and diameter of 13 mm. Then, the tablets were immersed in the MCT in an optical glass cuvette. Deionized water (2 μL) was gently placed on the surface of the tablets by the tip of a bent needle. After reaching equilibrium, the images of droplets were recorded and the contour of imaged drop was simulated with the Laplace–Young equation to acquire $\theta_{o/w}$. All the measurements were carried out in triplicate.

2.5. Field Emission Scanning Electronic Microscopy (FE-SEM)

The morphology of the complex nanoparticles was observed with a field emission scanning electron microscope (FE-SEM, SU8010, Hitachi). The samples were put on a double-sided adhesive coated with a thin layer of gold and measured under 20.0 kV acceleration voltage. (18)

2.6. Droplet Size and Zeta-Potential

The droplet size and size distribution were measured after preparation of emulsions for 12 h with a laser scattering size analyzer (LS230, Beckman Coulter, USA). The samples were diluted with deionized water at 3000 rpm until an obscuration rate between 8% and 12% was obtained. The optical properties were given as follows: a refractive index of 1.52 for MCT and absorption of 0.001 and a refractive index of 1.33 for the dispersant (deionized water). (16) The volume-area (D4,3) average diameters were calculated using eq 1

$$D_{4,3} = \frac{\sum n_i d_i^4}{\sum n_i d_i^3}$$

$$(1)$$

n_i is the number of particles with a diameter of d_i.

The zeta-potential of droplets was determined by measuring the direction and velocity of droplet movement in a well-defined electric field using a Zeta sizer NanoZS90 (Malvern Instruments, Worcestershire, UK). Emulsions were diluted to a final oil droplet concentration of 0.005 wt % with pH-adjusted deionized water (pH 4.0) to minimize multiple scattering effects. The data were collected from at least 10 sequential readings per sample after 120 s of equilibration and calculated by the instrument using the Smoluchowski model. (16) All measurements were performed in triplicate.

2.7. Physicochemical Stability of β-Carotene-Loaded Pickering Emulsions

2.7.1. Effect of UV Radiation

The photostability of β-carotene in Pickering emulsions against UV photolysis was analyzed. (3) Briefly, 15 g of fresh sample was placed into a transparent glass vial. Then, the sample was put in a cabinet with controlled light (0.68 W/m2, 45 °C, QSun, Q-Lab Corporation, Ohio, USA) for up to 8 h. The retention rate of β-carotene was plotted against time. All experiments were performed in triplicate.

2.7.2. Effect of Thermal Treatment

The emulsions were incubated in a water bath (85 °C) for 60 min and then cooled down to 25 °C. The retention rate of β-carotene was determined after thermal treatment. (8)

2.7.3. Effect of pH

The effect of pH on the emulsion stability was assessed. (22) The fresh emulsions were adjusted to pH 2.5, 6.0, and 8.5 using either 0.1 M NaOH or 0.1 M HCl solution.

2.7.4. Effect of Ionic Strength

The fresh emulsions were mixed with different weights of NaCl powder for 2 h to assure complete dissolution. NaCl concentrations in different emulsions were adjusted to 10, 50, and 100 mM. (22)

2.7.5. Effect of Storage Time

After the preparation of emulsions, fresh emulsions were stored at 55 °C for 4 weeks. The droplet size and retention rate of β-carotene in emulsions were measured at regular storage periods (1, 7, 14, 21, and 28 days). β-Carotene content was determined by our reported method. (18) Briefly, β-carotene in emulsions was extracted three times with a mixture of 1 mL ethanol and 3 mL of n-hexane. Then, absorbance at 450 nm was measured with a UV-1800 UV–vis spectrophotometer (Shimadzu, Japan).

2.8. Confocal Laser Scanning Microscopy (CLSM)

CLSM (Zeiss780, Germany) was performed to visualize the interfacial structure of emulsion droplets. The emulsions were stained with a mixed fluorescent dye solution consisting of Nile blue (0.1%) and Nile red (0.1%). Then, the dyed emulsions were deposited on concave confocal microscope slides and gently covered with a cover slip. (13) Nile blue was used to stain the ZPNPs, and Nile red was applied to dye the oil phase. The CLSM was operated using two laser excitation sources: an argon/krypton laser at 488 nm (Nile red) and a helium neon laser (He–Ne) at 633 nm (Nile blue).

2.9. Cryo-scanning Electron Microscopy (Cryo-SEM)

Through the cryo-SEM technique, the sample is vitrified with liquid nitrogen and maintained at a low temperature, which can preserve the emulsion structure in a frozen state and allow them to remain stable during the observation. (23) The interfacial structures of Pickering emulsions were observed by cryo-SEM. The samples were placed on an aluminum platelet and then transferred to a cryo-preparation system (PP3010T, Quorum Inc., UK) to flash-freeze the samples in liquid nitrogen slush followed by high vacuum sublimation of unbound water. The samples were freeze-fractured in the cryo-preparation chamber, coated with platinum. Then, the images were captured by using an SEM (Helios NanoLab G3 UC, FEI, USA).

2.10. *In Vitro* Digestion Analysis, Free Fatty Acid Release, and Bioaccessibility of β-Carotene

This study used a standardized *in vitro* gastrointestinal model with some modifications: (24)

For the stomach phase, 20 mL of the emulsion was mixed with 20 mL of simulated gastric fluid containing 0.0032 g/mL pepsin to mimic gastric digestion. The pH was adjusted to 2.0, and the sample was then swirled at 150 rpm for 1 h. For the small intestine phase, 20 mL of gastric digesta was transferred into a 100 mL glass beaker and then adjusted to pH 7.0. Thereafter, 20 mL of simulated intestinal fluid containing 5 mg/mL bile salt, 0.4 mg/mL pancreatin, and 3.2 mg/mL lipase was mixed with digesta in a reaction vessel. The pH was adjusted to 7.0, and the samples were held under continuous vibration at 150 rpm for 2 h to mimic small intestine digestion.

The degree of lipolysis was measured through the amount of free fatty acids (FFA) released. The amount of 0.25 M NaOH required to neutralize the released FFA through lipid digestion was determined using a pH-stat automatic titration unit (Metrohm, Switzerland, 916 Ti-Touch). The amount of FFA released was determined as the percentage of FFA (%) released during the digestion time using eq 2: (25)

$$\text{FFA}(\%) = \frac{V_{\text{NaOH}} m_{\text{NaOH}} M_{\text{lipid}}}{2 W_{\text{lipid}}} \times 100\%$$

$$(2)$$

where V_{NaOH} and m_{NaOH} represent the volume (L) and concentration (M) of NaOH solution needed to neutralize the FFA, respectively, and W_{lipid} and M_{lipid} represent the initial mass (g) and molecular mass (g·mol⁻¹) of the triacylglycerol oil, respectively.

The bioaccessibility of β-carotene was determined after the intestinal digestion. (3) Part of the digesta was processed by using a high-speed centrifuge at 15,000 rpm for 60 min at 4 °C. The micelle phase containing the solubilized β-carotene was collected. The content of β-carotene extracted from the initial emulsion and micelle fraction was determined according to the method described in 2.7.5. The bioaccessibility (%) of β-carotene was calculated by eq 3 below

$$\text{bioaccessibility}(\%) = \frac{C_{\text{micelle}}}{C_{\text{initial emulsion}}} \times 100\%$$

$$(3)$$

where C_{micelle} and $C_{\text{initial emulsion}}$ are the contents of β-carotene in the micelle fraction and the initial emulsion.

2.11. Statistical Analysis

All the measurements were repeated three times, and the data obtained were average values of triplicate determinations, which were subjected to statistical analysis of variance using SPSS 18.0 for Windows (SPSS Inc., Chicago, USA). Statistical differences were determined by one-way analysis of variance (ANOVA) with Duncan's post hoc test, and least significant differences ($p < 0.05$) were accepted among the treatments.

3. Results and Discussion

3.1. Characteristics of ZCPs

ZCPs showed a spherical shape with a uniform size (Figure 1A). A slight aggregation among the particles occurred due to the process of freeze-drying. The mean hydrodynamic size and zeta-potential of ZCPs were 381.1 ± 3.9 nm and 27.43 ± 0.58 mV, respectively. The isoelectric point (pI) of zein is around pH 6.2, (18) and therefore, ZCPs showed the positive electrical charge at pH 4.0, which provided sufficient steric and electrical repulsion against droplet coalescence once adsorbed onto the interface of Pickering emulsions. (5,26) Interfacial wettability is another key factor for the adsorption of Pickering stabilizers and can be evaluated by measuring the contact angle ($\theta_{o/w}$) of particles. (5) As shown in Figure 1B, the $\theta_{o/w}$ of ZCPs was 103.7 ± 1.1°, indicating the inherent hydrophobicity of ZCPs, which may induce bridging flocculation when ZCPs existed alone. (27)
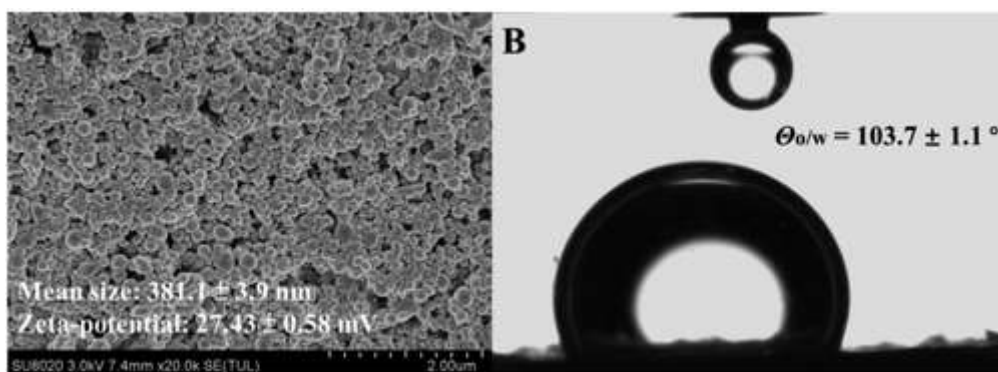
Figure 1. Morphology (A) and interfacial wettability (B) of ZCPs.

3.1.1. Fundamental Characteristics of Pickering Emulsions

Among all the emulsions, the ZCP-stabilized Pickering emulsion showed the largest droplet size (Figure 2A). This result suggested that although the particle-covered interface could provide electrostatic repulsion, the hydrophobic attraction between ZCPs promoted droplet aggregation and led to the emulsion destabilization. With the addition of PGA into the ZCP-covered interface, there was a significant ($p < 0.05$) decrease in the droplet size, indicating that the presence of PGA improved the emulsion stability and reduced the droplet aggregation. Previous studies also reported the synergistic effect between particles and emulsifiers in the emulsion stabilization. (28) It was worth noting that the droplet size of ZCPs/PGA became much smaller than that of ZCPs/Rha. The pKa of PGA is around 3.5, (29) and therefore, PGA carried substantial negative charge as an anionic polysaccharide at pH 4.0. When PGA was adsorbed to the particle-occupied interface, the droplet surface might form a more diffuse interfacial layer compared to the individual particle-stabilized interface. (3) The thickened interface could provide extra steric stability of the emulsion. With the addition of Rha, ZCPs and Rha could competitively adsorb onto the interface, reducing the stability of Pickering emulsions. (19,30) Meanwhile, Rha might adsorb to the particle surface through hydrophobic attraction, elevating the hydrophobicity of the particles and promoting particle aggregation. (27).
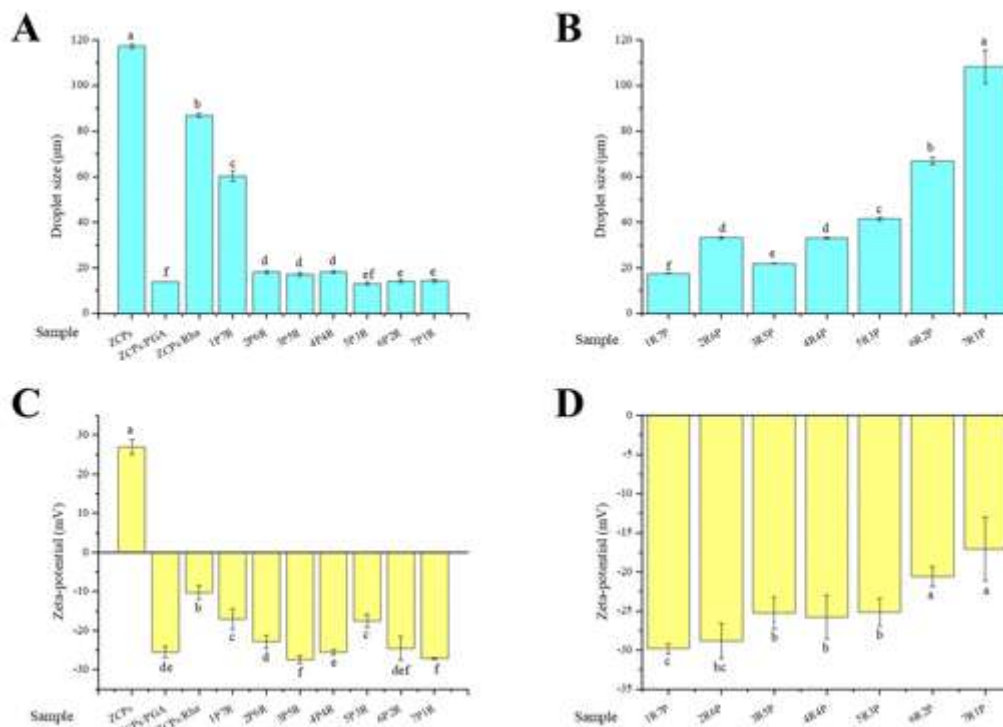
Figure 2. Droplet size of Pickering emulsions using PGA as a second layer and Rha as a third layer (A). Droplet size of Pickering emulsions using Rha as a second layer and PGA as a third layer (B). Zeta-potential of Pickering emulsions using PGA as a second layer and Rha as a third layer (C). Zeta-potential of Pickering emulsions using Rha as a second layer and PGA as a third layer (D).

When ZCPs, PGA, and Rha coexisted at the interface, the addition sequence and mass ratio of PGA and Rha showed significant effects on the droplet size. When PGA was added first and then Rha, as the mass ratio of PGA to Rha increased, the droplet size decreased quickly and reached a plateau. From 2P6R to 7P1R, the droplet size of Pickering emulsions remained constant with rising PGA level. This result again proved that when PGA and Rha coexisted on the particle-covered interface, PGA played a major role in stabilizing the emulsions, even at the low level of PGA. Figure 2B shows the impact of

PGA to Rha mass ratio on the emulsion droplet size when Rha was added first. Similarly, when the Rha level was increased, the droplet size increased continuously. The difference was that when Rha was added first, the droplet size immediately rose as the PGA level decreased from its highest level, which increased much faster than the droplet size of Pickering emulsions stabilized with PGA as a second layer. This phenomenon revealed that PGA had a much better stabilizing effect on the emulsion as the inner layer of the interface than the outer layer at its low levels. The low level of PGA in the outer layer of the interface might cause bridging flocculation between the droplets, which led to the larger droplet size as the PGA level declined. (16)

Figure S1A,B shows the droplet size distribution of different emulsions. Except for ZCPs/Rha and 1P7R, the droplet size of other emulsions showed a unimodal distribution (Figure S1A). Due to the strong hydrophobicity and large size of the particles, the ZCP-stabilized droplets obviously aggregated and coalesced. At the higher level of Rha, ZCPs and Rha could competitively adsorb onto the interface, which caused part of the particles to desorb from the interface. Part of Rha could enter into the aqueous phase and emulsify part of the lipid. Similarly, when Rha was in the inner layer and PGA was in the outer layer, the Pickering emulsions stabilized by the complex interface showed obvious flocculation at a higher proportion of Rha (Figure S1B). As the level of PGA increased, the droplet size of the emulsions gradually decreased, interpreting that the adsorption of PGA enhanced the repulsive force between the droplets to prevent emulsion coalescence. (16)

Figure 2C,D demonstrates the zeta-potential of the droplets in different emulsions. Undoubtedly, the ZCP-stabilized Pickering emulsion exhibited high positive electrical charge. With the incorporation of PGA or Rha, the surface charge carried by the droplets changed from positive to negative. It was observed that ZCPs/PGA showed a higher zeta-potential than ZCPs/Rha (Figure 2C). When the mass ratio of PGA to Rha was increased, the negative charge carried by the droplets was gradually increased, verifying that the presence of PGA could provide sufficient electrostatic repulsion against droplet aggregation. (13,22)

Figure S2 shows the visual appearance of different Pickering emulsions, which was consistent with their droplet sizes. It was observed that ZCPs/PGA exhibited a uniform and stable state without creaming, despite the phase separation that occurred in both ZCPs and ZCPs/Rha, which confirmed that the addition of PGA into the particle-laden interface prevented lipid droplets from aggregation. When ZCPs, PGA, and Rha coexisted at the interface, a similar phenomenon of phase separation only was observed in 1P7R, 6R2P, and 7R1P, which exactly accorded with their larger droplet sizes. This phenomenon proved that regardless of addition sequence of PGA and Rha, when the mass ratio of PGA and Rha was lower, the interfacial layer was incapable of providing the sufficient protection against droplet aggregation.

3.2. Environmental Stability

3.2.1. Physical Stability

The influence of interfacial composition on the physical stability of different emulsions was investigated through imposing centrifugal force. Among all the emulsions, ZCP-stabilized Pickering emulsion exhibited the highest instability index due to its largest droplet size. Compared to ZCPs/Rha, ZCPs/PGA showed much better physical stability, even better than the emulsions co-stabilized by ZCPs, PGA, and Rha (Figure 3A). Figure 3B demonstrates the physical stability of Pickering emulsions when PGA was added first and then Rha. At the low mass ratio of PGA to Rha, Pickering emulsions remain stable. When the PGA proportion was increased, the stability of the emulsions was gradually reduced until it reached the minimum (5P3R). Nevertheless, when the mass ratio of PGA to Rha was elevated

to a higher value, the instability index reversed to decrease greatly, which was similar to that of ZCPs/PGA. According to previous reports, after the biopolymer completely occupied the droplet surface, excessive biopolymer entered into the continuous phase and caused a depleting effect. (31,32) As its level was increased continuously, PGA entered into an aqueous phase and induced depletion flocculation between the droplets, resulting in the destabilization of the emulsions. (32) Meanwhile, the emulsion viscosity gradually increased, and the interaction between PGA and droplets could transform from depletion flocculation to depletion stabilization, improving the emulsion stability. (32).
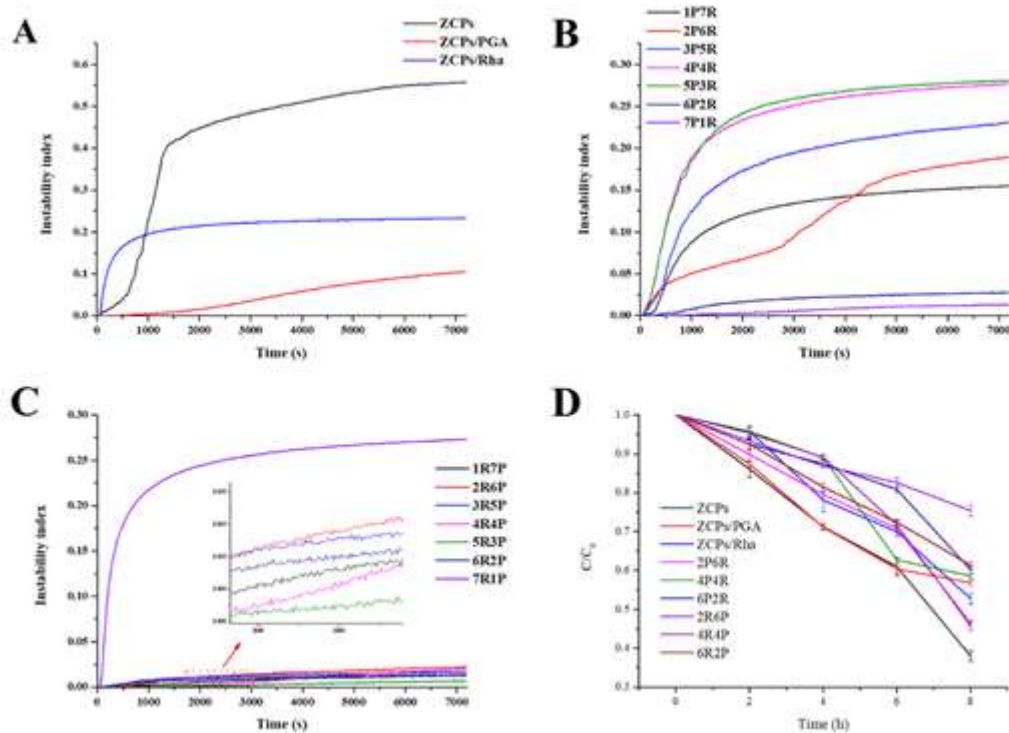
Figure 3. Physical stability of Pickering emulsions stabilized by ZCPs, ZCPs/PGA, and ZCPs/Rha (A). Physical stability of Pickering emulsions using PGA as a second layer and Rha as a third layer (B). Physical stability of Pickering emulsions using Rha as a second layer and PGA as a third layer (C). Photostability of β-carotene entrapped in Pickering emulsions (D).

When Rha was added first and then PGA, most of the Pickering emulsions exhibited excellent physical stability (Figure 3C). The combination of particles and PGA was more effective than the combination of particles and Rha to stabilize the interface. To our surprise, even though the droplet size of emulsions became larger with the outer layer of PGA, they showed better stability with the exception of 7R1P. This result indicated that PGA in the outer layer of the interface was more likely to enter into the aqueous phase, resulting in the enhanced viscosity and depletion stabilization. (31) When PGA lied on the outer layer of the interface, a more diffuse and thicker interfacial layer might be generated. When excessive Rha was added to the interface covered by ZCPs, it could induce competitive displacement between particles and the surfactant, causing the desorption and aggregation of ZCPs, thereby disrupting the steric and electrostatic repulsion between the droplets. (28) The phenomenon was consistent with many previous studies on the interactions between particles and surfactants at the interface. (28,30).

3.2.2. Photostability

Among all the emulsions, β-carotene entrapped in the ZCP-stabilized emulsion degraded most quickly under exposure to UV light (Figure 3D). The photostability of β-carotene was improved slightly with the incorporation of PGA and Rha into the particle-laden interface. Unlike the physical stability of the emulsions, the photostability of β-carotene in ZCPs/PGA scarcely showed a significant advantage over ZCPs/Rha. When ZCPs, PGA, and Rha coexisted at the interface, 2R6P showed the best protection for β-carotene against UV radiation, which reached the highest retention rate of 75.39 ± 1.51% after 8 h. Compared with other recent studies, the Pickering emulsions with complex interfaces showed some advantages in resisting the chemical degradation of β-carotene under light. (3,33) Wei *et al.* (2020) used the particles and lactoferrin to co-stabilize the Pickering emulsion and β-carotene entrapped remained around 80% after 4 h light treatment. (3) Liu *et al*. (2016) reported that β-carotene remained 70% in the emulsion stabilized by chlorogenic acid–lactoferrin–polydextrose conjugates after 8 h of UV radiation. (33) In addition, using Rha as the inner layer of interfaces and increasing the content of PGA enhanced the retention rate of β-carotene. This phenomenon interpreted that Rha could fill the gap between the particles at the interface, which reduced the direct access of light to the droplet surface. Meanwhile, when PGA was in the outer layer, the diffuse interfacial layer further reduced the penetration of light, effectively improving the photostability of β-carotene in oil droplets. (3)

3.2.3. pH Stability

The influence of different pH values (2.0, 6.0, and 9.0) on the droplet size and zeta-potential of different Pickering emulsions was investigated (Figure 4). It was noted that all the emulsions remained relatively stable at pH 2.0. Although the zeta-potential was greatly reduced or even close to 0 except ZCPs, the droplet size of all the emulsions remained constant. The interpretation was that the interface composed of particles, PGA, and Rha provided sufficient steric repulsion to prevent droplet aggregation, even without electrostatic repulsion between the droplets. The largest increase in droplet size occurred in the ZCP-stabilized Pickering emulsion as the pH was shifted to 6.0, which was because the pH was close to the pI of zein (6.2). (34) The droplet size of other emulsions still remained stable, although the zeta-potential was increased. The same phenomenon still showed that no matter what addition sequence between PGA and Rha, the emulsion stability became better at the higher level of PGA. At pH 9.0, the droplet size of the ZCP-stabilized Pickering emulsion was decreased significantly ($p < 0.05$) compared to that at pH 6.0. The enhanced negative electrical charge strengthened the electrostatic repulsion against droplet aggregation. Nevertheless, the droplet size of the emulsions with complex interfaces was increased in an alkaline environment, accompanied by the increased zeta-potential. All of the three interfacial components (ZCPs, PGA, and Rha) carried massive negative charges, and the strong electrostatic repulsion separated the three emulsifiers from each other, especially PGA that carried the most negative charge. Therefore, at pH 9.0, a looser interfacial layer was formed by the mixed emulsifiers. The electrostatic repulsion between the emulsifiers caused stronger competitive instabilization on the interface rather than adsorption onto the droplet surface. (35) The presence of emulsifiers disrupted the interaction between the particles at the interface, which disturbed the interfacial layer and increased the probability of interfacial rupture. (2,9) As reported by previous studies, the presence of surfactants was detrimental to the emulsion stability based on the orogenic displacement model. (2,35) When Rha was added first and then PGA, the droplet size of the emulsions was larger than that of the emulsions using PGA as a second layer. Moreover, strong electrostatic repulsion between ZCPs and PGA might cause the part of PGA to detach from the interface and enter into the aqueous phase, reducing the steric hindrance between the droplets and enhancing the depleted flocculation. (22)
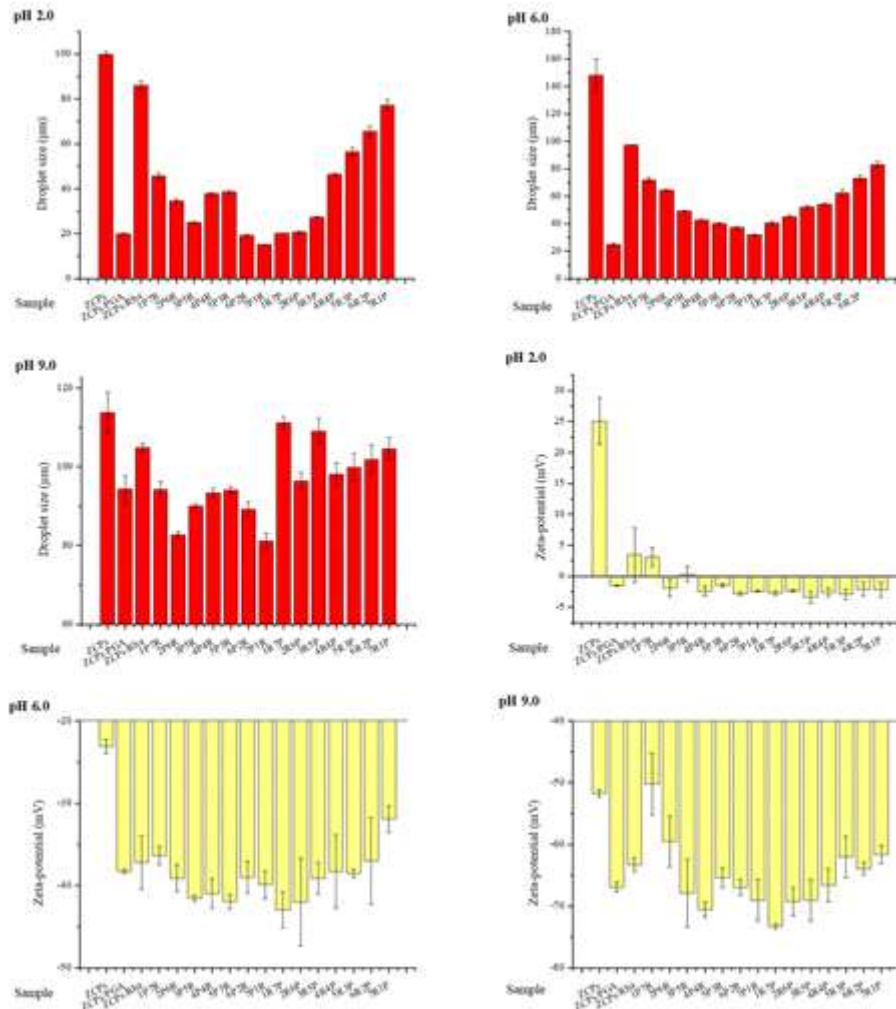
Figure 4. Influence of different pH values on the droplet size and zeta-potential of Pickering emulsions co-stabilized by ZCPs, PGA, and Rha.

3.2.4. Ionic Strength Stability

As shown in Figure 5, the stability of Pickering emulsions with different interfacial compositions was investigated under different ionic strengths (200–800 mM). At 200 mM, the droplet size of most of the emulsions remained constant without aggregation except ZCPs and ZCPs/Rha, revealing their excellent stability. It was observed that the zeta-potential of ZCPs and ZCPs/Rha was decreased below |15| mV, which could promote the droplet flocculation without sufficient electrostatic repulsion. (16) The composite ZCPs/PGA interfacial layer provided more negative charge and prevented aggregation between particles due to hydrophobic attraction. With the concentration of NaCl increasing from 200 to 800 mM, the droplet size was increased slightly, which was attributed to reduced electrostatic repulsion between droplets owing to electrostatic screening. It was worth noting that there was a larger increase in the droplet size of ZCPs/PGA than ZCPs/Rha, suggesting that the interfacial layer composed of ZCPs and PGA was more susceptible to the magnitude of charge than that of ZCPs and Rha. When ZCPs, PGA, and Rha co-located at the interface, the higher PGA content was liable to induce the droplet aggregation with increased droplet size due to charge neutralization. This phenomenon interpreted that the weakening of the electrostatic attraction between ZCPs and PGA promoted PGA

to detach from the interfacial layer into the aqueous phase, which reduced the repulsion between the droplets and induced depletion flocculation. (32,36)
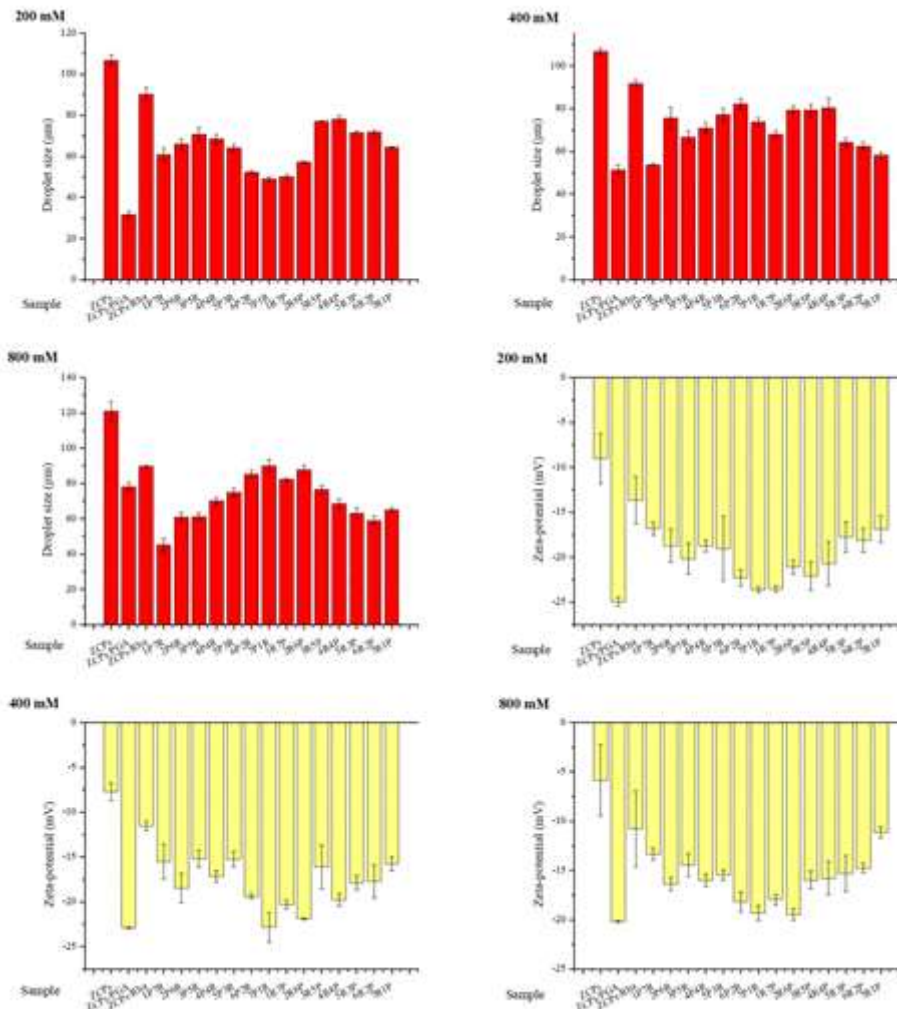
Figure 5. Impact of different ionic strengths on the droplet size and zeta-potential of Pickering emulsions co-stabilized by ZCPs, PGA, and Rha.

3.3. Morphological Observation

In this study, we showed the CLSM and cryo-SEM images corresponding to each sample to comprehensively explore the microstructures of different Pickering emulsions. The droplets were severely aggregated and deformed in the Pickering emulsion stabilized by ZCPs alone (Figure 6). Although a large number of particles occupied the surface of oil droplets, they could not effectively prevent emulsion coalescence. This result was mainly attributed to the strong hydrophobicity of ZCPs, which caused the droplets to flocculate and coalesce. With the incorporation of PGA, the droplet size of Pickering emulsions was decreased greatly. The droplets were uniformly distributed in ZCPs/PGA without aggregation, deformation, and coalescence. Meanwhile, it was observed that the particle morphology on the droplet surface became blurred, forming a smooth interfacial film. This observation interpreted that excessive PGA was added to the particle-laden interface, not only co-adsorbed with the particles onto the droplet surface but also formed the outer layer outside the particle film. (16,32) Compared to ZCPs/PGA, there existed slight aggregation between the droplets in

ZCPs/Rha. It was found that many droplets shared a common interface. There might be two reasons for this phenomenon: On one hand, the adsorption of Rha onto the droplet surface could disturb the interaction between particles and reduce the interfacial tension. (13) At a high level of Rha, the competitive displacement of the surfactant with particles at the interface caused some particles to be replaced, which reduced the interfacial elasticity of the emulsion and made the droplet surface easily disrupted and unstable. (28) On the other hand, part of the surfactant might be adsorbed on the particle surface, thereby inducing bridging flocculation between droplets. Binks and Rodrigues (2007) investigated the interactions between particles and surfactants and their effects on the stability of Pickering emulsions. They found that the double phase inversion of the emulsions stabilized by a mixture of particles and surfactants was induced by the surfactant concentration. (30) As shown in the cryo-SEM images of ZCPs/Rha, densely distributed pits could be observed on the droplet surface, which verified that the particles and surfactant underwent a competitive displacement that caused the particles to detach from the interface. In a previous study, we utilized three different surfactants and particles to stabilize Pickering emulsions and found that the particles could be replaced at high levels of surfactant, which was consistent with some other studies. (13,28,37)
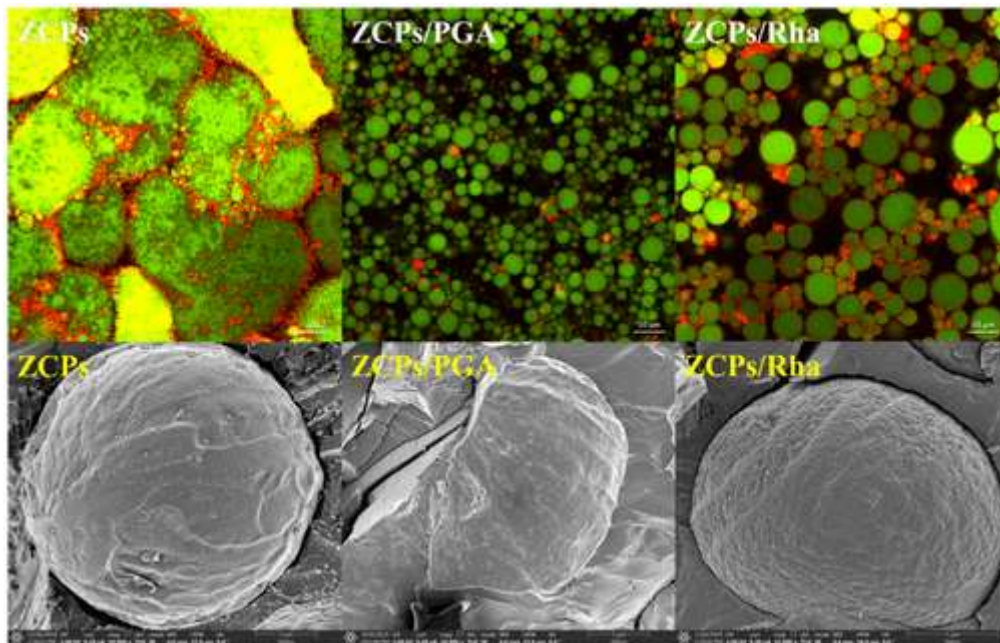
Figure 6. CLSM images and cryo-SEM microstructures of Pickering emulsion stabilized by ZCPs solely, ZCPs and PGA, and ZCPs and Rha.

Figure 7 demonstrates the morphological features and interfacial structures of Pickering emulsions co-stabilized by ZCPs, PGA, and Rha. Through CLSM, it was observed that the emulsion was inhomogeneous and part of the droplets were aggregated at the lower mass ratio of PGA and Rha. As the mass ratio of PGA and Rha continued to increase, the emulsion became more uniform with a smaller droplet size. Through observing the interfacial structure, many small pores appeared on the droplet surface of 1P7R and 7R1P, indicating that a higher level of Rha and particles competitively adsorbed to the interface. When the mass ratio between PGA and Rha increased, the interfacial pores gradually disappeared and the particles tended to aggregate. Interestingly, when the PGA level reached the maximum, the addition sequence of PGA and Rha caused a huge difference in the interfacial structures of 1R7P and 7P1R. 7P1R showed a very smooth surface of the droplets, and the spherical particles and interfacial pores could be hardly observed. Nevertheless, the interface film with

an obvious network and bridging structures between the particles was observed in 1R7P. When PGA was added first and then Rha, the negatively charged PGA would be electrostatically deposited on the positively charged particle film, completely covering the surface of the droplets. Subsequently, a small amount of Rha was difficult to penetrate through the interfacial layer with the bilayer structure of the particles and PGA; therefore, they could be only adsorbed on the outer layer of the PGA film or bound to PGA chains to form the complexes through hydrophobic and electrostatic attraction. When Rha was added first and then PGA, Rha could be adsorbed onto the surface of the droplets competitively with the particles, thereby causing orgenic displacement of the particles at the interface. (35,38) Moreover, the interactions between ZCPs and Rha might promote cross-linking between the particles, which was consistent with our previous results. (3,13) Meanwhile, Rha and PGA could promote the formation of an elastic network of aggregated close-packed particles through the mechanism of orogenic displacement and polymer bridging. (2,14,32) Both the particle–polymer mixture and the particle–surfactant mixture played important roles in stabilizing Pickering emulsions and had a profound impact on the macroscopic features of the emulsions and subsequent digestion behavior in the gastrointestinal tract.
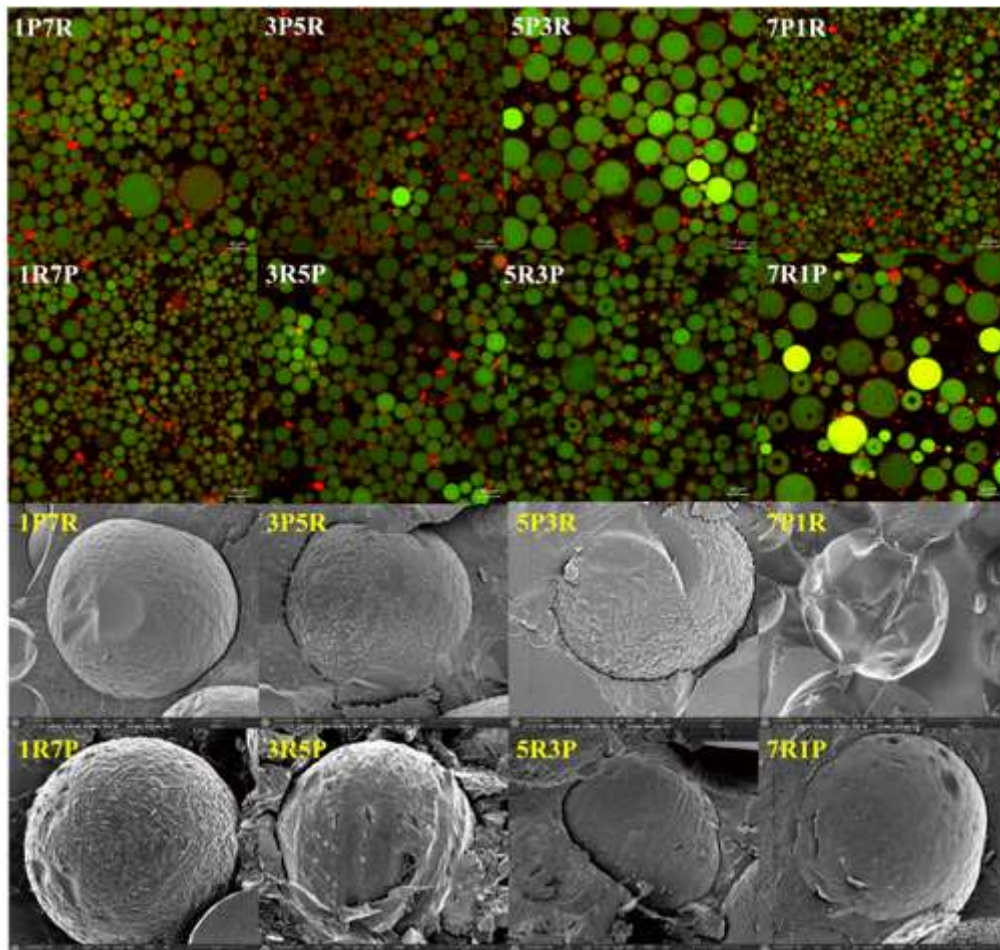
Figure 7. CLSM images and cryo-SEM microstructures of Pickering emulsions co-stabilized by ZCPs, PGA, and Rha.

3.4. Rheological Properties

3.4.1. Apparent Viscosity

The ZCP-stabilized Pickering emulsion showed the highest viscosity among all the emulsions (Figure 8A). As discussed above, the particles attached at the interface possessed strong hydrophobicity, causing a serious droplet aggregation due to the hydrophobic attraction. The flocculation of the droplets further led to emulsion coalescence with the enhanced viscosity. (8,39) Additionally, ZCPs/Rha exhibited a high viscosity similar to ZCP-stabilized Pickering emulsion. With the adsorption of the high level of Rha into the particle-laden interface, although the emulsion became more uniform and the degree of aggregation was reduced, part of the droplets still aggregated to form a network structure. This phenomenon might be ascribed to the replacement of the particles by surfactant molecules at the interface, which caused the particles to aggregate and form the bridging between the droplets. (30) Rha adsorbed on the surface of the particles could enhance the hydrophobicity of the particles, thus promoting the particle aggregation and the droplet flocculation. (13,27) Additionally, unadsorbed Rha could form micelles in the aqueous phase, and these micelles could cause depletion flocculation between droplets. (40) With the incorporation of PGA, the viscosity of ZCPs/PGA was lower than that of ZCPs. Through the observation of CLSM and cryo-SEM, it was found that PGA reduced the droplet size and inhibited the droplet aggregation, which adsorbed on the outer layer of the droplets and formed a smooth interfacial film. This result unraveled that the addition of PGA did not cause obvious competitive adsorption with particles. In addition, PGA could effectively stabilize the emulsion interface without excessive PGA entering the aqueous phase to cause depletion flocculation between the droplets. (32,36)
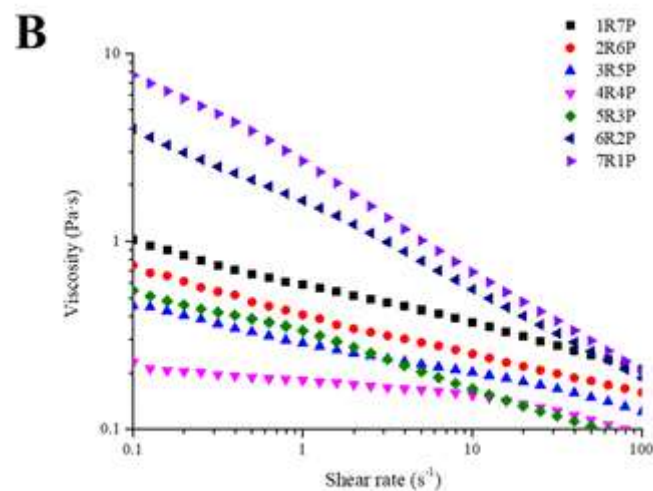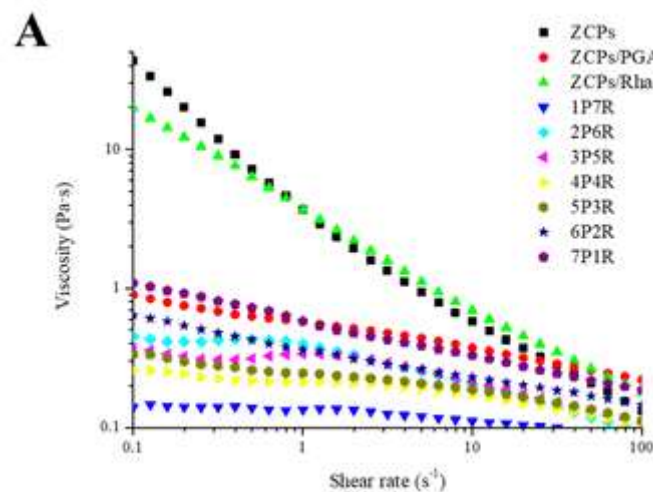
Figure 8. Apparent viscosity of Pickering emulsions using PGA as a second layer and Rha as a third layer (A). Apparent viscosity of Pickering emulsions using Rha as a second layer and PGA as a third layer (B).

In the presence of ZCPs, PGA, and Rha, the emulsion viscosity became much smaller than those of ZCPs and ZCPs/Rha. When PGA was added first and then Rha, the emulsion viscosity was decreased sharply and reached the minimum at the lowest concentration of PGA (1P7R). This phenomenon could be because PGA and Rha at this mass ratio formed the polymer–surfactant mixtures through certain intermolecular interactions. For instance, electrostatic interactions between the polar head groups of the surfactant and the polymer backbone as well as hydrophobic attraction between surfactant tails and the hydrophobic backbone of polymers were the dominant factors to contribute to the formation of the complexes. The interactions between the polymer and surfactant could reduce the competitive displacement between particles and emulsifiers and diminish the formation of micelles in the aqueous phase, which further reduced the interfacial particle aggregates and droplet aggregation driven by depletion flocculation. (2) With the rise in the mass ratio of PGA to Rha, the viscosity of the emulsion gradually increased and finally approximated to that of ZCPs/PGA.

Figure 8B shows that 7R1P exhibited the highest viscosity among the emulsions when Rha was added first and then PGA, which was consistent with that of ZCPs/Rha. It was noted that the viscosity of 7R1P was much higher than that of 1P7R although they had the same interfacial composition but different structures, indicating that PGA used as the outer layer showed greater influence on the bulk property than that as the inner layer. This phenomenon revealed that when Rha was added first, it could adsorb onto the droplet surface competitively with the particles, interact with particles directly, or form micelles in the aqueous phase, hindering its binding to PGA. (3,13) With the continuous rise in PGA level, the emulsion viscosity was gradually decreased, reached the minimum in 4R4P, and reversely increased at a higher level of PGA. Excessive PGA entering the continuous phase might form a network structure and cause depletion flocculation between the droplets, thereby increasing the viscosity of the emulsion. (22)

3.4.2. Viscoelastic Properties

As shown in Figure 9A, the *G′* was much greater than *G″* in ZCPs and ZCPs/Rha in the full frequency range, which represented the formation of an elastic particulate gel-like structure. (22) With the incorporation of PGA into the particle-covered interface, the *G′* of ZCPs/PGA was greatly decreased and entangled with *G″*, indicating a transition of the emulsions from a solid- to liquid-like behavior. This result indicated that the droplets easily formed the bridges and aggregated in ZCPs and ZCPs/PGA, and PGA could inhibit the formation of bridges between the interfaces stabilized by particles or particle–surfactant complexes, hindering the aggregation of emulsion droplets.

In the presence of particles, a biopolymer, and a surfactant, both *G′* and *G″* of different emulsions were kept at a relatively low level when PGA was added first as a second layer and then Rha as a third layer, which was similar to that of ZCPs/PGA (Figure 9B). In addition, the G′ was very close to the *G″*, revealing that the emulsions mainly showed the liquid characteristics without the obvious aggregation. (41)Figure 9C presents the viscoelastic properties of the emulsions when Rha was added first and then PGA. It could be observed that when the mass ratio between Rha and PGA was lower, both *G′* and *G″* of Pickering emulsions were similar and low, which was consistent with the emulsions using the PGA as the inner layer and Rha as the outer layer. When the Rha level gradually increased, *G′* increased obviously and became much higher than *G″*. When Rha was used as the inner layer, the rising Rha level disrupted the stability of the interfacial film and promoted the droplet flocculation. The increased Rha concentration could promote the aggregation and desorption of the particles at the interface through competitive displacement and further lead to flocculation and coalescence

between droplets, which was consistent with their droplet sizes. (13,30,35) Moreover, the adsorption of negatively charged surfactants on positively charged particles could partially screen the repulsion between the particles in addition to increasing their hydrophobicity. (30) Therefore, the emulsions formed from particle–surfactant mixtures became gel-like with highly flocculated droplets.
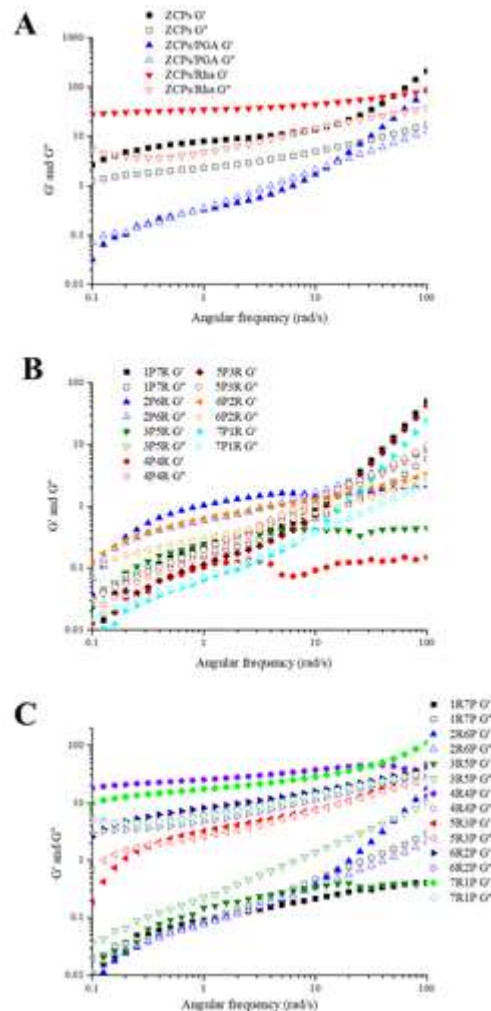
Figure 9. Viscoelasticity of Pickering emulsions stabilized by ZCPs, ZCPs/PGA, and ZCPs/Rha (A). Viscoelasticity of Pickering emulsions using PGA as a second layer and Rha as a third layer (B). Viscoelasticity of Pickering emulsions using Rha as a second layer and PGA as a third layer (C).

3.5. *In Vitro* Gastrointestinal Digestion of β-Carotene-Loaded Pickering Emulsions

3.5.1. Microstructure

The microstructural alteration of Pickering emulsions in simulated gastrointestinal tract was monitored through CLSM. The droplets aggregated and coalesced to varying degrees after the gastric digestion for 60 min (Figure 10). Among different Pickering emulsions, the most serious aggregation between the droplets occurred in ZCPs/Rha, which might be related to the peptic hydrolysis of ZCPs at the interface. The proteolysis process could cause the aggregation of the particles or detachment of the particles from the droplets, which further undermined the stability of Pickering emulsions. Nevertheless, it was observed that ZCPs/PGA and other Pickering emulsions co-stabilized by ZCPs, PGA, and Rha remained relatively stable, which suggested that the addition of PGA provided the sufficient repulsion against droplet aggregation although the electrostatic repulsion between them

was negligible without net charge at pH 2.0. After digestion in the simulated small intestine, most of the lipid droplets were slightly disaggregated. In addition, the morphology of the emulsion droplets was changed from a spherical to irregular shape, and the protein particle film originally adsorbed on the surface of droplets basically disappeared. This phenomenon was due to the substantial negative charge of PGA in the neutral environment, which caused the droplets to separate due to electrostatic repulsion. In the small intestinal phase, the protein particles were digested and part of the lipids was hydrolyzed.
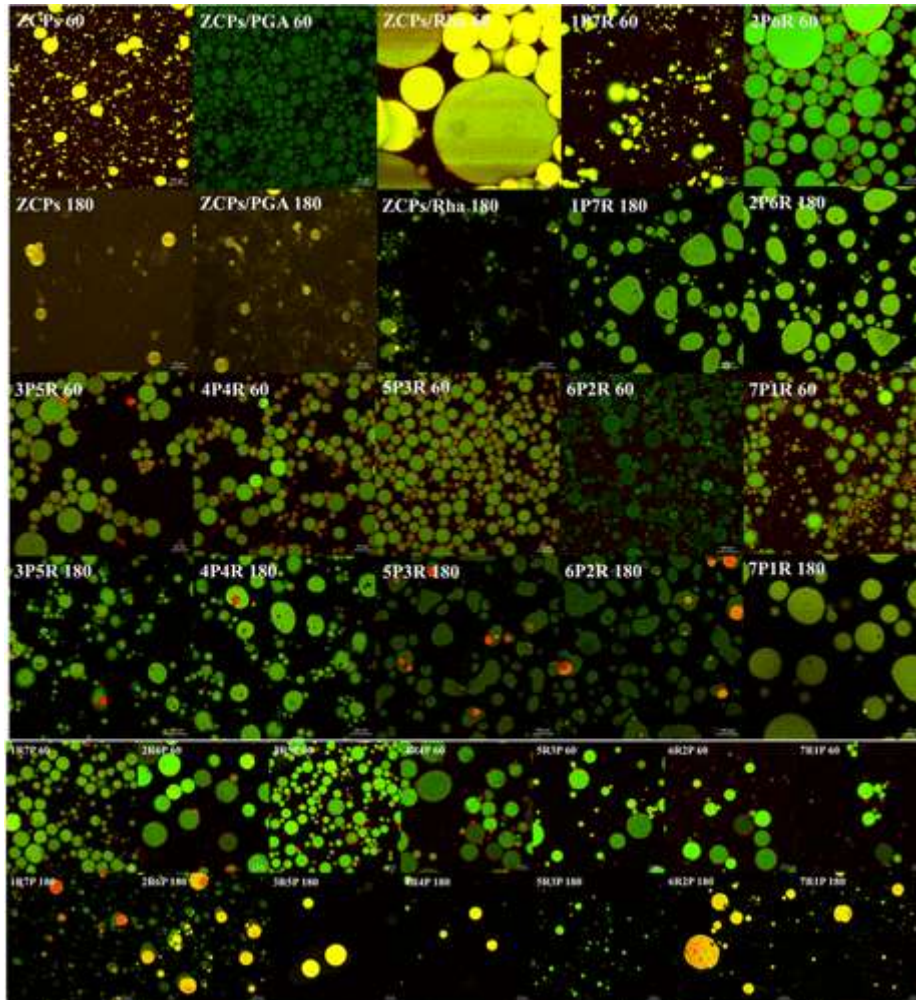
Figure 10. Microstructures of Pickering emulsions co-stabilized by ZCPs, PGA, and Rha at different digestion times.

3.5.2. Droplet Size

During the gastric digestion, the droplet size of different Pickering emulsions was elevated slightly when PGA was added first and then Rha (Figure 11A). The droplet size distribution of different emulsions after gastric digestion is shown in Figure S3A. Among all the Pickering emulsions, the highest increase in droplet size occurred in ZCPs/Rha, indicating that a serious aggregation appeared between droplets. As aforementioned, the addition of Rha could cause orogenic displacement of the particles, leading to interfacial destabilization and droplet aggregation. The hydrolysis of zein further disintegrated the particle film with the aid of pepsin, which promoted the emulsion coalescence. The Pickering emulsions using complex interfaces exhibited the excellent gastric stability in the presence

of PGA. These results testified that the coating of PGA restricted the access of pepsin to binding sites of ZCPs, which protected ZCPs from proteolysis. In addition, the high bulk viscosity of Pickering emulsions hindered the diffusion of pepsin to the proteinaceous sides of the particles at a higher PGA level. (12)
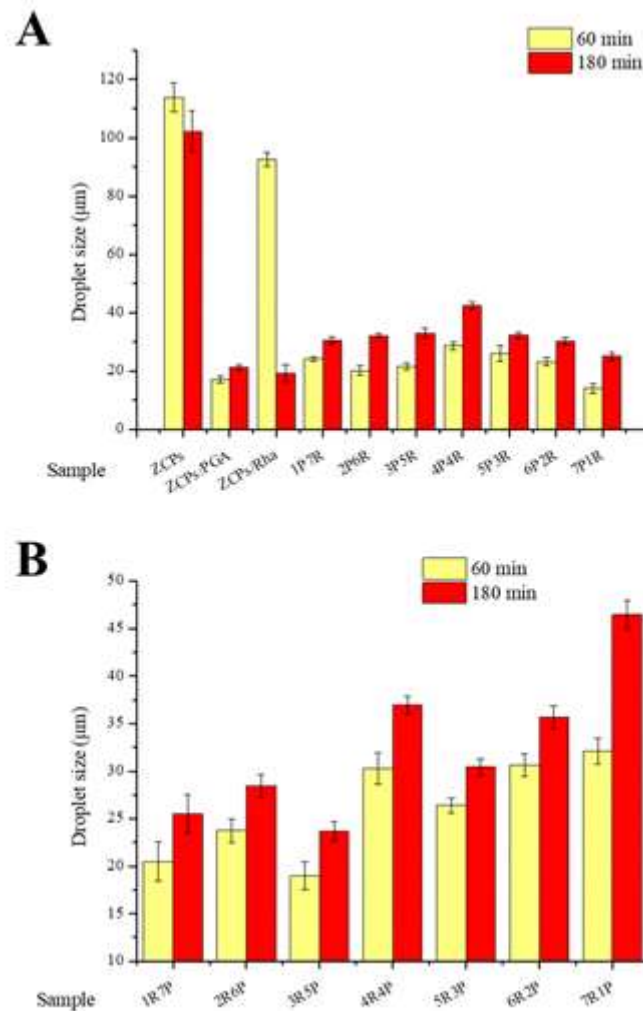
Figure 11. Digestion time dependence of the droplet size of Pickering emulsions using PGA as a second layer and Rha as a third layer (A). Digestion time dependence of droplet size of Pickering emulsions using Rha as a second layer and PGA as a third layer (B).

After the gastric digesta passed into the small intestine, there was an obvious decrease in the droplet size of ZCPs and ZCPs/Rha. Figure S3B demonstrates the droplet size distribution of different emulsions after small intestinal digestion. The presence of pancreatin, bile salts, and lipase might destroy the aggregation between droplets and facilitate the re-emulsification of droplets. In addition, lipolytic products could accumulate at the interface and affect the droplet bridging. Nevertheless, in most of the Pickering emulsions with complex interfaces, the droplet size was slightly increased, which was reasonably caused by the digestion of proteins and lipids. The bile salts, lipases, and subsequent digestive products could replace the partial components (ZCPs, PGA, and Rha) of complex interfaces; however, they were incapable of forming new viscoelastic films to stabilize the emulsions against coalescence. (42)

Figure 11B shows the droplet size of Pickering emulsions stabilized by complex interfaces after gastrointestinal digestion for 60 and 180 min. It was observed that the droplet size of all the Pickering emulsions was increased through the digestion in the small intestinal phase, indicating that the digestion of proteins and lipids undermined the stability of interfacial layers. Meanwhile, the increase in droplet size of Pickering emulsions was reduced with rising PGA level. The presence of PGA layer sterically and electrostatically hindered the permeation of bile salts and digestive enzymes through the interfacial layers and the adsorption onto the droplet surface, which might inhibit the coalescence of Pickering emulsions.

3.5.3. Lipid Digestion

As demonstrated in Figure 12A, the ZCP-stabilized Pickering emulsion showed the highest FFA release (19.46%) among all the Pickering emulsions, which was much lower than conventional emulsions stabilized by a single biopolymer or surfactant. (15) Li and McClements used different low-molecular-weight emulsifiers (Tween 20, Tween 80, and SDS) to stabilize nanoemulsions at the same concentration (1.5%, w/w) and lower oil fraction (10%, w/w), which released around 30% FFA after in vitro gastrointestinal digestion using a pH-stat method. (15) In another study, the researchers reported the OSA-modified-starch-stabilized nanoemulsions that release around 100% FFA during intestinal digestion for 2 h. (43) These results interpreted that the particle-laden interface could delay the lipid digestion in a more efficient way compared to an individual surfactant or biopolymer, which was because the particles adsorbed on the droplet surface were more difficult to be displaced by bile salts or lipases in the small intestine phase than conventional emulsifiers due to the energy barrier. (5)

Nevertheless, the practical applications of Pickering emulsions solely stabilized by solid particles in delaying lipid digestion cannot be faultless. Above all, the particles could scarcely occupy the droplet surface completely due to their steric and electrostatic repulsion, and therefore, there were substantial interfacial gaps between the adsorbed particles. The incorporation of PGA and Rha reduced the release rates of FFA to 15.64% and 18.05% in ZCPs/PGA and ZCPs/Rha, respectively (Figure 12A). Due to the more flexible molecular structure and smaller molecular weight, Rha entered into the interfacial gaps more feasibly than PGA and co-adsorbed with the particles on the surface of droplets, thereby inhibiting the adsorption of bile salts and lipase to the droplet surface through interfacial gaps. On the other hand, PGA could cover the outer layer of the particle film by electrostatic deposition. Owing to the massive negative charge of PGA, its presence could produce strong electrostatic repulsion with negatively charged bile salts, thereby hindering the access of bile salts and lipases.

In the presence of ZCPs, PGA, and Rha, Pickering emulsions stabilized by the complex interfaces showed the excellent capacity of delaying lipolysis. When PGA was added first and then Rha, the release rate of FFA was continuously decreased from 18.38% (1P7R) to 9.01% (7P1R) with increasing PGA proportion (Figure 12A). The experimental results showed that although Rha could restrict the adsorption of bile salts and lipase by occupying interfacial gaps, the adsorption of PGA delayed lipolysis more efficiently by forming steric and electrostatic repulsion as the outer layer of droplets. To our surprise, when Rha was added first and then PGA, the Pickering emulsions stabilized by ZCPs, Rha, and PGA followed the opposite law in the release of FFA (Figure 12B). With the increase in Rha level, the release rate of FFA in the Pickering emulsions using Rha as a second layer was gradually reduced from 8.84% (1R7P) to 2.83% (6R2P), although there was a slight rise in 7R1P (3.32%). It was noted that the release rate of FFA in Pickering emulsions using Rha as a second layer became much lower than PGA. This phenomenon could be explained by two mechanisms: On one hand, when PGA existed in the outer layer (using Rha as a second layer), its molecular chain could extend into the aqueous phase

more adequately and increase the bulk viscosity, thereby slowing down the movement of digestive substances (bile salts and lipases) in the small intestine phase due to gelling and bile acid binding properties of weak gels with interpenetrating polymer networks. (4) On the other hand, Rha could fill more interfacial gaps between the particles as the inner layer and form a network bridge between the adsorbed particles, thereby inhibiting the bile salts and lipases from contacting the oil droplet surface. (13,42) Additionally, the increased Rha could also be adsorbed on the surface of the particles and increase the hydrophobicity of the particles, thereby promoting particle aggregation and flocculation between droplets. This phenomenon reduced the surface area accessible to bile salts and lipase, thereby retarding the hydrolysis of lipids.
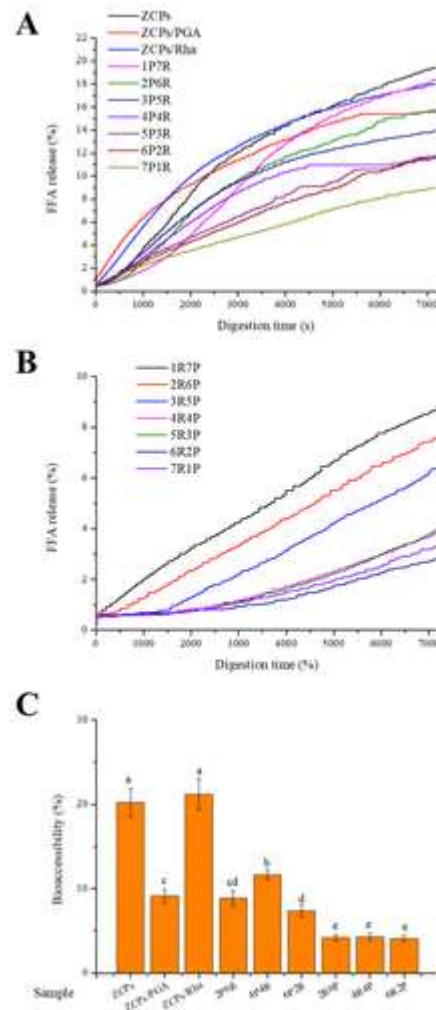
Figure 12. Digestion time dependence of FFA release (%) from Pickering emulsions using PGA as a second layer and Rha as a third layer (A). Digestion time dependence of FFA release (%) from Pickering emulsions using Rha as a second layer and PGA as a third layer (B). Bioaccessibility of β-carotene entrapped in different Pickering emulsions co-stabilized by ZCPs, PGA, and Rha (C).

3.5.4. Bioaccessibility of β-Carotene

The release profile of nutraceuticals from food matrix in gastrointestinal fluids is the premise of determining their bioaccessibility. The release and solubilization of lipophilic nutrients occur for the most part in the small intestine, which are affected by several exogenous factors, such as properties

of nutrients, food processing, interfacial composition, and so forth. (44) The solubilization capacity of the mixed micelles formed is the determining factor of bioaccessibility by calculating the concentration of lipophilic nutraceuticals in the micellar phase. (45)

In the present study, the bioaccessibilities of β-carotene in ZCPs and ZCPs/Rha were 20.21 ± 1.69% and 21.20 ± 1.82%, respectively, which were much higher than those of other Pickering emulsions (Figure 12C). Although the FFA release rate of ZCPs/PGA was similar to those of ZCPs and ZCPs/Rha, the bioaccessibility of β-carotene in ZCPs/PGA was only 9.12 ± 0.79%. The incorporation of PGA might restrict the formation of micelles by slowing down the diffusion rate of bile salts in the intestinal lumen, which might be attributed to gelling and bile acid binding properties of weak gels with interpenetrating polymer networks. In addition, the hydrophobic attraction could facilitate FFA and β-carotene released to bind to the back bone of PGA molecules, which restricted them to solubilize into the mixed micelles. (4) In terms of Pickering emulsions when PGA was added first and then Rha, the bioaccessibility of β-carotene was close to that in ZCPs/PGA. Nevertheless, the release rate of FFA in ZCPs/PGA was higher than that in the Pickering emulsions co-stabilized by ZCPs, PGA, and Rha. The inconsistency indicated that the presence of Rha was more advantageous to facilitate the formation of mixed micelles than PGA, which showed a positive impact on the solubility capacity of β-carotene. Nevertheless, when Rha was added first and then PGA, the interfacial composition showed insignificant influence on the bioaccessibility of β-carotene (∼4.2%) in Pickering emulsions co-stabilized by ZCPs, PGA, and Rha, which was much lower than that of Pickering emulsions using PGA as a second layer and Rha as a third layer. This result proved that Rha could fill more interfacial gaps between ZCPs as the inner layer and form a network bridge between the particles, subsequently delaying lipolysis and FFA release, which further diminished the fraction of nutrients incorporated into the micellar phase. (46) Meanwhile, when PGA was in the outer layer of the interface, it could more fully form a network structure to hinder the adsorption of bile salts and lipase and the diffusion of mixed micelles, thereby reducing the transport of β-carotene from the intestinal lumen to the mucosal layer.

4. Conclusions

The physicochemical stability, interfacial structure, and *in vitro* gastrointestinal digestion of particle, particle–biopolymer, particle–surfactant, and particle–surfactant–biopolymer complex interface-stabilized Pickering emulsions were investigated. It was observed that the stability of Pickering emulsion stabilized solely by ZCPs was very poor. When the particles were combined with a biopolymer (PGA) and surfactant (Rha) as surface-active agents, there seemed to be a synergistic effect on improving the environmental stability of Pickering emulsions. It is demonstrated for the first time the use of triple emulsifier for the development of the novel Pickering emulsion for delivery of lipophilic nutraceuticals. These findings underlined the importance of controlling the addition sequence and mass ratio of multiple stabilizers, which showed the enhanced stability and controlled lipid digestion of particle–biopolymer–surfactant-stabilized Pickering emulsions over than those stabilized by particles, particle–biopolymer, and particle–surfactant mixtures. The novel Pickering emulsions could be applied in foods as well as pharmaceuticals for controlling lipid digestion or targeted nutrient delivery purposes. This research is of great significance to the stabilizing mechanism and practical application of the complex interfaces in Pickering emulsions. In the future, the metabolic pathways and nutrient absorption of Pickering emulsion in the human digestive tract need to be explored *ex vivo* and *in vivo*.

Supporting Information

Notes

Acknowledgments

References

1 McClements, D. J.; Gumus, C. E. Natural Emulsifiers — Biosurfactants, Phospholipids, Biopolymers, and Colloidal Particles: Molecular and Physicochemical Basis of Functional Performance. Adv. Colloid Interface Sci. 2016, 234, 3– 26, DOI: 10.1016/j.cis.2016.03.002

2 Pugnaloni, L. A.; Dickinson, E.; Ettelaie, R.; Mackie, A. R.; Wilde, P. J. Competitive Adsorption of Proteins and Low-Molecular-Weight Surfactants: Computer Simulation and Microscopic Imaging. Adv. Colloid Interface Sci. 2004, 107, 27– 49, DOI: 10.1016/J.CIS.2003.08.

3 Wei, Y.; Tong, Z.; Dai, L.; Wang, D.; Lv, P.; Liu, J.; Mao, L.; Yuan, F.; Gao, Y. Influence of Interfacial Compositions on the Microstructure , Physiochemical Stability , Lipid Digestion and β -Carotene Bioaccessibility of Pickering Emulsions. Food Hydrocolloids 2020, 104, 105738, DOI: 10.1016/j.foodhyd.2020.105738

4 Maldonado-Valderrama, J.; Wilde, P.; Macierzanka, A.; Mackie, A. The Role of Bile Salts in Digestion. Adv. Colloid Interface Sci. 2011, 165, 36– 46, DOI: 10.1016/J.CIS.2010.12.002

5 Binks, B. P. Particles as Surfactants—Similarities and Differences. Curr. Opin. Colloid Interface Sci. 2002, 7, 21– 41, DOI: 10.1016/S1359-0294(02)00008-0

6 Xiao, J.; Wang, X.; Perez Gonzalez, A. J.; Huang, Q. Kafirin Nanoparticles-Stabilized Pickering Emulsions: Microstructure and Rheological Behavior. Food Hydrocolloids 2016, 54, 30– 39, DOI: 10.1016/J.FOODHYD.2015.09.008

7 Sarkar, A.; Ademuyiwa, V.; Stubley, S.; Esa, N. H.; Goycoolea, F. M.; Qin, X.; Gonzalez, F.; Olvera, C. Pickering Emulsions Co-Stabilized by Composite Protein/ Polysaccharide Particle-Particle Interfaces: Impact on in Vitro Gastric Stability. Food Hydrocolloids 2018, 84, 282– 291, DOI: 10.1016/j.foodhyd.2018.06.019

8 Wei, Y.; Yu, Z.; Lin, K.; Yang, S.; Tai, K.; Liu, J.; Mao, L.; Yuan, F.; Gao, Y. Fabrication, Physicochemical Stability and Microstructure of Coenzyme Q10 Pickering Emulsions Stabilized by Resveratrol Loaded Composite Nanoparticles. J. Agric. Food Chem. 2020, 68, 1405, DOI: 10.1021/acs.jafc.9b06678

9 Binks, B. P.; Desforges, A.; Duff, D. G. Synergistic Stabilization of Emulsions by a Mixture of Surface-Active Nanoparticles and Surfactant. Langmuir 2007, 23, 1098– 1106, DOI: 10.1021/la062510y

10 Dickinson, E. Mixed Biopolymers at Interfaces: Competitive Adsorption and Multilayer Structures. Food Hydrocolloids 2011, 25, 1966– 1983, DOI: 10.1016/J.FOODHYD.2010.12.001

11 Sarkar, A.; Zhang, S.; Holmes, M.; Ettelaie, R. Colloidal Aspects of Digestion of Pickering Emulsions: Experiments and Theoretical Models of Lipid Digestion Kinetics. Adv. Colloid Interface Sci. 2019, 263, 195– 211, DOI: 10.1016/j.cis.2018.10.002

12 Sarkar, A.; Li, H.; Cray, D.; Boxall, S. Composite Whey Protein–Cellulose Nanocrystals at Oil-Water Interface: Towards Delaying Lipid Digestion. Food Hydrocolloids 2018, 77, 436– 444, DOI: 10.1016/j.foodhyd.2017.10.020

13 Wei, Y.; Tong, Z.; Dai, L.; Ma, P.; Zhang, M.; Liu, J.; Mao, L.; Yuan, F.; Gao, Y. Novel Colloidal Particles and Natural Small Molecular Surfactants Co-Stabilized Pickering Emulsions with Hierarchical Interfacial Structure: Enhanced Stability and Controllable Lipolysis. J. Colloid Interface Sci. 2020, 563, 291– 307, DOI: 10.1016/J.JCIS.2019.12.085

14 Murray, B. S.; Durga, K.; Yusoff, A.; Stoyanov, S. D. Stabilization of Foams and Emulsions by Mixtures of Surface Active Food-Grade Particles and Proteins. Food Hydrocolloids 2011, 25, 627– 638, DOI: 10.1016/j.foodhyd.2010.07.025

15 Li, Y.; McClements, D. J. Inhibition of Lipase-Catalyzed Hydrolysis of Emulsified Triglyceride Oils by Low-Molecular Weight Surfactants under Simulated Gastrointestinal Conditions. Eur. J. Pharm. Biopharm. 2011, 79, 423– 431, DOI: 10.1016/j.ejpb.2011.03.019

16 Wei, Y.; Sun, C.; Dai, L.; Mao, L.; Yuan, F.; Gao, Y. Novel Bilayer Emulsions Costabilized by Zein Colloidal Particles and Propylene Glycol Alginate, Part 1: Fabrication and Characterization. J. Agric. Food Chem. 2018, 67, 1197– 1208, DOI: 10.1021/acs.jafc.8b03240

17 Patel, A. R.; Velikov, K. P. Zein as a Source of Functional Colloidal Nano- and Microstructures. Curr. Opin. Colloid Interface Sci. 2014, 19, 450– 458, DOI: 10.1016/J.COCIS.2014.08.001

18 Wei, Y.; Sun, C.; Dai, L.; Zhan, X.; Gao, Y. Structure, Physicochemical Stability and in Vitro Simulated Gastrointestinal Digestion Properties of β-Carotene Loaded Zein-Propylene Glycol Alginate Composite Nanoparticles Fabricated by Emulsification-Evaporation Method. Food Hydrocolloids 2018, 81, 149– 158, DOI: 10.1016/j.foodhyd.2018.02.042

19 Bai, L.; McClements, D. J. Formation and Stabilization of Nanoemulsions Using Biosurfactants: Rhamnolipids. J. Colloid Interface Sci. 2016, 479, 71– 79, DOI: 10.1016/J.JCIS.2016.06.047

20 Liu, F.; Zhu, Z.; Ma, C.; Luo, X.; Bai, L.; Decker, E.; Gao, Y.; McClements, D. J. Fabrication of Concentrated Fish Oil Emulsions Using Dual-Channel Microfluidization: Impact of Droplet Concentration on Physical Properties and Lipid Oxidation. J. Agric. Food Chem. 2011, 64, 9532– 9541, DOI: 10.1021/acs.jafc.6b04413

21 Wei, Y.; Li, C.; Zhang, L.; Dai, L.; Yang, S.; Liu, J.; Mao, L.; Yuan, F.; Gao, Y. Influence of Calcium Ions on the Stability, Microstructure and in Vitro Digestion Fate of Zein-Propylene Glycol Alginate-Tea Saponin Ternary Complex Particles for the Delivery of Resveratrol. Food Hydrocolloids 2020, 106, 105886, DOI: 10.1016/j.foodhyd.2020.105886

22 Wei, Y.; Sun, C.; Dai, L.; Mao, L.; Yuan, F.; Gao, Y. Novel Bilayer Emulsions Costabilized by Zein Colloidal Particles and Propylene Glycol Alginate. 2. Influence of Environmental Stresses on Stability and Rheological Properties. J. Agric. Food Chem. 2019, 67, 1209– 1221, DOI: 10.1021/acs.jafc.8b04994

23 Sriamornsak, P.; Thirawong, N.; Cheewatanakornkool, K.; Burapapadh, K.; Sae-Ngow, W. Cryo-Scanning Electron Microscopy (Cryo-SEM) as a Tool for Studying the Ultrastructure during Bead Formation by Ionotropic Gelation of Calcium Pectinate. Int. J. Pharm. 2008, 352, 115– 122, DOI: 10.1016/J.IJPHARM.2007.10.038

24 Minekus, M.; Alminger, M.; Alvito, P.; Ballance, S.; Bohn, T.; Bourlieu, C.; Carrière, F.; Boutrou, R.; Corredig, M.; Dupont, D.A Standardised Static in Vitro Digestion Method Suitable for Food-an International Consensus. Food Funct. 2014, 5, 1113– 1124, DOI: 10.1039/c3fo60702j

25 Li, Y.; McClements, D. J. New Mathematical Model for Interpreting PH-Stat Digestion Profiles: Impact of Lipid Droplet Characteristics on in Vitro Digestibility. J. Agric. Food Chem. 2010, 58, 8085– 8092, DOI: 10.1021/jf101325m

26 Dickinson, E. Biopolymer-Based Particles as Stabilizing Agents for Emulsions and Foams. Food Hydrocolloids 2017, 68, 219– 231, DOI: 10.1016/J.FOODHYD.2016.06.024

27 French, D. J.; Taylor, P.; Fowler, J.; Clegg, P. S. Making and Breaking Bridges in a Pickering Emulsion. J. Colloid Interface Sci. 2015, 441, 30– 38, DOI: 10.1016/J.JCIS.2014.11.032

28 Xu, M.; Jiang, J.; Pei, X.; Song, B.; Cui, Z.; Binks, B. P. Novel Oil-in-Water Emulsions Stabilised by Ionic Surfactant and Similarly Charged Nanoparticles at Very Low Concentrations. Am. Ethnol. 2018, 57, 7738– 7742, DOI: 10.1002/anie.201802266

29 Sun, C.; Wei, Y.; Li, R.; Dai, L.; Gao, Y. Quercetagetin-Loaded Zein–Propylene Glycol Alginate Ternary Composite Particles Induced by Calcium Ions: Structure Characterization and Formation Mechanism. J. Agric. Food Chem. 2017, 65, 3934– 3945, DOI: 10.1021/acs.jafc.7b00921

30 Binks, B. P.; Rodrigues, J. A. Double Inversion of Emulsions by Using Nanoparticles and a Di-Chain Surfactant. Am. Ethnol. 2007, 46, 5389– 5392, DOI: 10.1002/anie.200700880

31 Ji, S.; Walz, J. Y. Synergistic Effects of Nanoparticles and Polymers on Depletion and Structural Interactions. Langmuir 2013, 29, 15159– 15167, DOI: 10.1021/la403473g

32 Dickinson, E. Exploring the Frontiers of Colloidal Behaviour Where Polymers and Particles Meet. Food Hydrocolloids 2016, 52, 497– 509, DOI: 10.1016/j.foodhyd.2015.07.029

33 Liu, F.; Wang, D.; Xu, H.; Sun, C.; Gao, Y. Physicochemical Properties of β-Carotene Emulsions Stabilized by Chlorogenic Acid–Lactoferrin–Glucose/Polydextrose Conjugates. Food Chem. 2016, 196, 338– 346, DOI: 10.1016/J.FOODCHEM.2015.09.047

34 Shukla, R.; Cheryan, M. Zein: The Industrial Protein from Corn. Ind. Crops Prod. 2001, 13, 171– 192, DOI: 10.1016/S0926-6690(00)00064-9

35 Wilde, P.; Mackie, A.; Husband, F.; Gunning, P.; Morris, V. Proteins and Emulsifiers at Liquid Interfaces. Adv. Colloid Interface Sci. 2004, 108-109, 63– 71, DOI: 10.1016/J.CIS.2003.10.011

36 Firoozmand, H.; Murray, B. S.; Dickinson, E. Interfacial Structuring in a Phase-Separating Mixed Biopolymer Solution Containing Colloidal Particles. Langmuir 2009, 25, 1300– 1305, DOI: 10.1021/la8037389

37 Zou, S.; Yang, Y.; Liu, H.; Wang, C. Synergistic Stabilization and Tunable Structures of Pickering High Internal Phase Emulsions by Nanoparticles and Surfactants. Colloids Surfaces A Physicochem. Eng. Asp. 2013, 436, 1– 9, DOI: 10.1016/J.COLSURFA.2013.06.013

38 Mackie, A.; Wilde, P. The Role of Interactions in Defining the Structure of Mixed Protein–Surfactant Interfaces. Adv. Colloid Interface Sci. 2005, 117, 3– 13, DOI: 10.1016/J.CIS.2005.04.002

39 Dai, L.; Wei, Y.; Sun, C.; Mao, L.; McClements, D. J.; Gao, Y. Development of Protein-Polysaccharide-Surfactant Ternary Complex Particles as Delivery Vehicles for Curcumin. Food Hydrocolloids 2018, 85, 75– 85, DOI: 10.1016/j.foodhyd.2018.06.052

40 Wei, Y.; Yu, Z.; Lin, K.; Sun, C.; Dai, L.; Yang, S.; Mao, L.; Yuan, F.; Gao, Y. Fabrication and Characterization of Resveratrol Loaded Zein-Propylene Glycol Alginate-Rhamnolipid Composite Nanoparticles: Physicochemical Stability, Formation Mechanism and in Vitro Digestion. Food Hydrocolloids 2019, 95, 336– 348, DOI: 10.1016/j.foodhyd.2019.04.048

41 Dai, L.; Sun, C.; Wei, Y.; Mao, L.; Gao, Y. Characterization of Pickering Emulsion Gels Stabilized by Zein/Gum Arabic Complex Colloidal Nanoparticles. Food Hydrocolloids 2018, 74, 239– 248, DOI: 10.1016/J.FOODHYD.2017.07.040

42 Sarkar, A.; Zhang, S.; Holmes, M.; Ettelaie, R. Colloidal Aspects of Digestion of Pickering Emulsions: Experiments and Theoretical Models of Lipid Digestion Kinetics. Advances in Colloid and Interface Science. Elsevier B.V. January 1, 2019, pp. 195– 211, DOI: 10.1016/j.cis.2018.10.002 .

43 Lin, Q.; Liang, R.; Ye, A.; Singh, H.; Zhong, F. Effects of Calcium on Lipid Digestion in Nanoemulsions Stabilized by Modified Starch: Implications for Bioaccessibility of β-Carotene. Food Hydrocolloids 2017, 73, 184– 193, DOI: 10.1016/j.foodhyd.2017.06.024

44 Dima, C.; Assadpour, E.; Dima, S.; Jafari, S. M. Bioavailability of Nutraceuticals: Role of the Food Matrix, Processing Conditions, the Gastrointestinal Tract, and Nanodelivery Systems. Compr. Rev. Food Sci. Food Saf. 2020, 19, 954, DOI: 10.1111/1541-4337.12547

45 Sarkar, A.; Mackie, A. R. Engineering Oral Delivery of Hydrophobic Bioactives in Real-World Scenarios. Curr. Opin. Colloid Interface Sci. 2020, 48, 40– 52, DOI: 10.1016/j.cocis.2020.03.009

46 Yao, M.; Xiao, H.; McClements, D. J. Delivery of Lipophilic Bioactives: Assembly, Disassembly, and Reassembly of Lipid Nanoparticles. Annu. Rev. Food Sci. Technol. 2014, 5, 53– 81, DOI: 10.1146/annurev-food-072913-100350